PAPER ID: 0371
DOI: 10.18462/iir.compr.2021.0371

NUMERICAL ANALYSIS OF THE TRANSIENT COMPRESSIBLE FLUID FLOW IN THE PISTON-CYLINDER CLEARANCE OF AN OIL-FREE LINEAR COMPRESSOR

Claudio J. Santos, Thiago Dutra, Cesar J. Deschamps*
POLO Research Laboratories for Emerging Technologies in Cooling and Thermophysics
Federal University of Santa Catarina, CEP 88048-300, Florianopolis, SC, Brazil, deschamps@polo.ufsc.br

ABSTRACT

Oil-free linear compressors adopt aerostatic bearings to avoid metal contact between the piston and cylinder. Despite the small friction in the bearing, the gas flow in the piston-cylinder clearance can generate losses that decrease the compressor efficiency. The present paper reports a model developed to evaluate such losses and their effects on the volumetric and isentropic efficiencies. The transient compressible fluid flow in the gap is simulated with a commercial code based on the finite volume method, whereas the compression cycle in the cylinder is solved with an in-house code using a lumped model formulation. The model was employed to assess the compressor performance as a function of four parameters: compressor speed, piston oscillation amplitude, pressure ratio and radial clearance, It was found that the compressor efficiency is mainly reduced when the clearance dimension and pressure ratio are increased.

Keywords: Linear Compressor. Clearance. Leakage. Energy efficiency. Volumetric efficiency.

1. INTRODUCTION

Fig. 1 shows the main components and most important geometric parameters of an oil-free linear compressor driven by a magnet motor. The linear drive mechanism with a resonant spring allows the use of part of the kinetic energy of the system, reducing the current required in the motor and, therefore, the power input. The piston of a linear compressor is subjected to low side loads and metal contact can be avoided by feeding high-pressure refrigerant gas from the discharge chamber into the piston-cylinder clearance. The line located at a distance L_{instop}Linstop from the valve plate (Fig. 1b) represents the position around which the piston oscillates with an amplitude L_{amp}. Table 1 shows the values of the geometric parameters indicated in Fig. 1(b). The nominal piston-cylinder clearance is δ δ= 5 μm.

Most of the models developed to simulate linear compressors are comprised of submodels for the piston dynamics, compression cycle and leakage in the piston-cylinder clearance (Bradshaw et al., 2011; Jomde et al., 2018). In these models, the leakage in the piston cylinder clearance is analytically solved for a combined Couette-Poiseuille incompressible flow. However, this type of approach is not suitable for predicting the leakage of gas through the clearance due to presence of compressibility effects (Braga and Deschamps, 2017).

The effect of the aerostatic bearing formed by the piston-cylinder clearance on the oil-free compressor efficiency is not yet fully understood. This paper reports an assessment of the thermodynamic inefficiencies brought about by the transient compressible fluid flow in the piston-cylinder clearance of an oil-free linear compressor. The different sources of volumetric and isentropic inefficiencies in the piston-cylinder clearance are then identified and quantified for the baseline operating conditions, by using the convenient approach proposed by Perez-Segarra et al. (2005). A sensitivity analysis is then carried out to evaluate the effect of design parameters on these inefficiencies.

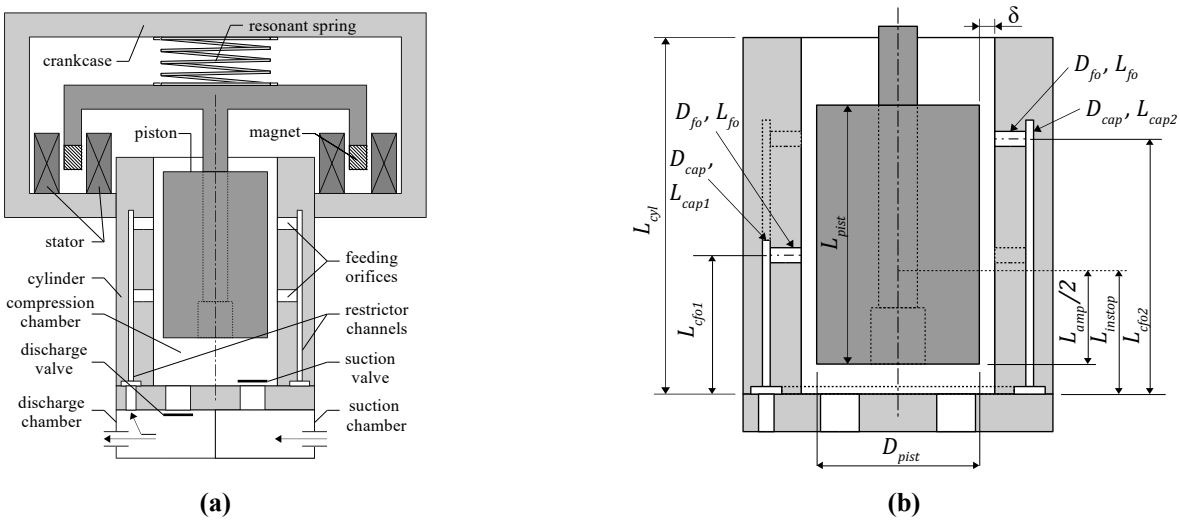

Figure 1: Schematics of the linear compressor: (a) main moving parts; (b) geometric parameters – piston at the TDC.

Table 1: Geometric parameters.

Parameter	Value	Parameter	Value	Parameter	Value
L_{pist}/L_{cyl}	0.82	L_{instop}/L_{cyl}	0.12	D_{fo}/L_{cyl}	$1.60\text{x}10^{-2}$
L_{cfo1}/L_{cyl}	0.42	L_{cap1}/D_{cap}	$5.15\text{x}10^{3}$	D_{cap}/L_{cyl}	$8.40\text{x}10^{-4}$
L_{cfo2}/L_{cyl}	0.78	L_{cap2}/D_{cap}	$6.53\text{x}10^{3}$	D_{pist}/L_{cyl}	0.31

2. SIMULATION MODEL

Three submodels were developed to form the simulation model adopted to analyze the inefficiencies in the piston-cylinder clearance of an oil-free linear compressor. These models take into account different phenomena: i) compression cycle in the cylinder; ii) transient compressible fluid flow in the piston cylinder clearance; and iii) compressible fluid flow through the restrictor channels. These submodels are detailed in the following sections.

2.1. Compression Chamber Model

The compression chamber model (CC) was developed via a lumped formulation for the mass and energy conservation equations. It should be mentioned that the convective heat transfer at the cylinder walls and pressure drop due to valves and mufflers were neglected, since the objective of this paper is to analyze the inefficiencies brought about solely by the leakage in the piston-cylinder gap. Leakage at the top clearance, $\dot{m}_{gtp}$, can occur in two directions, from the clearance towards the compression chamber and in the opposite direction, and it is calculated from the finite-volume model adopted for the clearance, as will be detailed in section 2.2. The indicated power and the mass flow rate predicted by the CC model are required to evaluate the thermodynamic inefficiencies.

2.2. Piston-Cylinder Model

The solution domain of the piston-cylinder clearance model (PCC) consists of the clearance region depicted in Fig. 1. The dimension of radial clearance is much smaller than the piston diameter. Therefore, curvature effects were disregarded, and the solution domain was simplified to the geometry of two parallel plates. The solution domain is further simplified due to planes of symmetry in the circumferential direction (Fig. 2).

The mass, momentum and energy conservation equations are required to solve the transient compressible fluid flow. The dynamic viscosity is obtained from the library REFPROP® v8.0. The hypothesis of ideal gas was

adopted and the viscous dissipation rate, Φ, was calculated at each time step from the results of velocity field. The governing equations were solved via the finite-volume method with the code Fluent v14. The boundary conditions for the flow are those indicated in Fig. 2. Simulations are initialized with the piston positioned at the top dead center (TDC). The velocity field is set to zero and the temperature field is set to 328.15K. At the TDC, interfaces a) and f) are submitted to condensing and evaporation pressure conditions, respectively. A linear variation in the pressure between these two surfaces is set as the initial condition.

2.3. Restrictor Channel Model

The restrictor channels are grooves positioned on the outer wall of the cylinder. The mass flow rate leaving the restrictor channels is estimated by assuming the hypothesis of laminar, isothermal compressible fluid flow, following Hülse and Prata (2016). The mass flow rate in each restrictor channel is provided as a boundary condition for the PCC model.

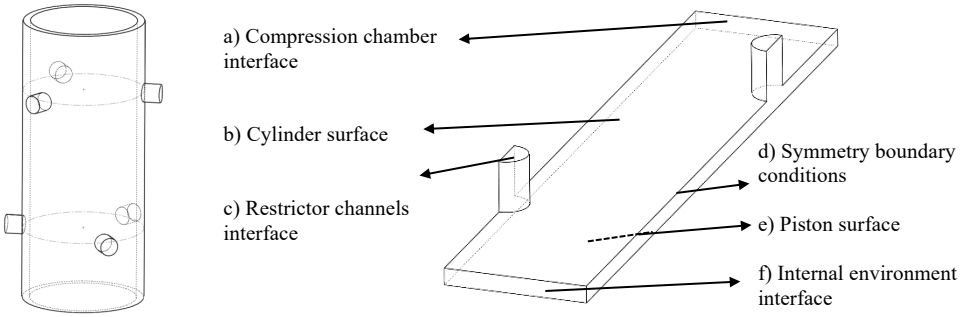

Figure 2: Piston-cylinder clearance solution domain.

3. ANALYSIS OF THERMODYNAMIC INEFFICIENCIES

In the following sections, a method is presented to identify the main volumetric and isentropic inefficiencies associated with the flow in the piston-cylinder clearance of a small oil-free linear compressor.

3.1. Volumetric Inefficiency

The mass flow rate at the entrance of the compression chamber ($\dot{m}_{in,i}$) can be written as a function of the ideal mass flow rate, $\dot{m}_{th} = \forall_{sw}\, \rho_{suc}\, f$, where $\forall_{sw}$ is the swept volume and ρ_{suc} is the gas density in the suction line, and reductions associated with different effects:

$$\dot{m}_{in,i} = \dot{m}_{th} - \left(1 - \eta_{v,idc}\right)\dot{m}_{th} - \dot{m}_{gtp(exp)} - \dot{m}_{gtp(suc)} - \left(\rho_{ini,comp} - \rho_{suc}\right) \forall_{BDC}\, f \qquad \text{Eq. (1)}$$

The second term on the right-hand side of Eq. (1) represents the reduction caused by the effect of the dead volume ($\eta_{v,idc}$). The terms $\dot{m}_{gtp(exp)}$ and $\dot{m}_{gtp(suc)}$ represent the mean flow rates through the piston top clearance during the expansion and suction processes, respectively. Positive values for $\dot{m}_{gtp(exp)}$ and $\dot{m}_{gtp(suc)}$ indicate that leakage occurs from the gap to the compression chamber, reducing the mass flow rate since a smaller amount of mass from the suction would enter the compression chamber. The last term of Eq. (1) is the loss due to the difference between the gas densities in the suction line and inside the cylinder at the beginning of the compression process ($\rho_{suc} - \rho_{ini,comp}$). The variable $\forall_{BDC}$ is the maximum volume of the compression chamber.

Fig. 3 shows a diagram of the mass and energy fluxes between different regions of the compressor. The mass flow rate through the piston skirt, $\dot{m}_{gsk}$, recirculates inside the compressor, reducing the actual mass flow rate provided by the compressor, $\dot{m}$. A mass balance in the suction environment, which corresponds to the region upstream of the compression chamber, indicates:

$$\dot{m} = \dot{m}_{in,i} - \dot{m}_{gsk} \qquad \text{Eq. (2)}$$

Substituting Eq. (2) into Eq. (1) and dividing the final expression by $\dot{m}_{th}$ gives:

$$\frac{\dot{m}}{\dot{m}_{th}} = \eta_{v,idc} - \frac{\dot{m}_{gtp,exp}}{\dot{m}_{th}} - \frac{\dot{m}_{gtp,suc}}{\dot{m}_{th}} - \frac{(\rho_{suc} - \rho_{ini,comp})\,\forall_{BDC}\,f}{\dot{m}_{th}} - \frac{\dot{m}_{gsk}}{\dot{m}_{th}} \quad \text{Eq. (3)}$$

The volumetric efficiency is the ratio between the actual and ideal mass flow rates ($\eta_v = \dot{m}/\dot{m}_{th}$). We introduce εv_k to represent the volumetric inefficiencies, i.e., the fraction of the total mass flow rate reduction due to a specific effect k ($\varepsilon v_k = \dot{m}_k/\dot{m}_{th}$). Hence, Eq. (3) can be written as:

$$\eta_v = \eta_{v,idc} - \varepsilon v_{gtp,exp} - \varepsilon v_{gtp,suc} - \varepsilon v_{sh} - \varepsilon v_{gsk} \quad \text{Eq. (4)}$$

where the terms εv_k are determined by the different models. The total volumetric inefficiency due to the flow in the piston-cylinder clearance is:

$$\varepsilon v = \varepsilon v_{gtp,exp} + \varepsilon v_{gtp,suc} + \varepsilon v_{sh} + \varepsilon v_{gsk} \quad \text{Eq. (5)}$$

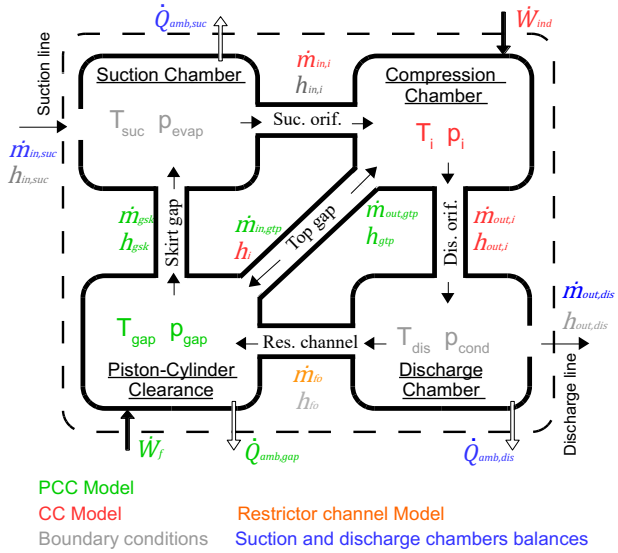

Figure 3: Interaction between the models.

3.2. Isentropic Inefficiency

The isentropic inefficiencies can be determined by calculating the amount of heat that should be withdrawn from the control volume (dashed line in Fig. 3) to make the entropy of the gas at the outlet equal to its entropy at the inlet. This means that the heat transfer rates indicated in Fig. 3 can be regarded as energy transfer rates that make the actual process different from the isentropic process.

Neglecting the losses of the electric motor and assuming that the bearing loss is due to the resistive force of the viscous friction on the piston, $\dot{W}_f$, the compressor power input is $\dot{W} = \dot{W}_{ind} + \dot{W}_f$, where $\dot{W}_{ind}$ is the indicated power. Thus, considering the energy balance in the control volume of Fig. 3:

$$\dot{W}_{ind} + \dot{W}_f + \dot{m}_{in,suc} h_{in,suc} = \dot{Q}_{amb,gap} + \dot{Q}_{amb,suc} + \dot{Q}_{amb,dis} + \dot{m}_{out,dis} h_{out,dis} \quad \text{Eq. (6)}$$

where $\dot{m}$ and h represent the mass flow rate and specific enthalpy at the inlet and outlet of the control volume. At the inlet, the evaporating pressure, p_{evap}, and the suction line temperature, T_{suc}, are prescribed. At the outlet, the reference thermodynamic state is established by assuming an isentropic compression process from the inlet condition (p_{evap} and T_{suc}) to the condensing pressure, p_{cond}. The discharge temperature is denoted by T_{dis}. Under stabilized operating conditions, the mass balance provides $\dot{m}_{in,suc} = \dot{m}_{out,dis} = \dot{m}$.

The term $\dot{Q}_{amb,gap}$ represents the heat transfer rate in the piston-cylinder clearance, which is calculated with the

PCC model for a prescribed wall temperature obtained from measurements. On the other hand, $\dot{Q}_{amb,suc}$ and $\dot{Q}_{amb,dis}$ are not actually the heat transfer rates at the walls of the suction and discharge systems, which are assumed adiabatic. In fact, $\dot{Q}_{amb,suc}$ and $\dot{Q}_{amb,dis}$ are determined from energy balances in the suction and discharge systems, respectively, so as to keep the specific entropy constant. The energy balance applied to the suction chamber is represented by

$$\dot{Q}_{amb,suc} = \dot{m}_{in,suc}\, h_{in,suc} + \dot{m}_{gsk}\, h_{gsk} - \dot{m}_{in,i}\, h_{in,i}. \quad \text{Eq. (7)}$$

where $\dot{m}_{gsk}$ and h_{gsk} are predicted with the PCC model and $\dot{m}_{in,i}$ is calculated with the CC model. The mass balance shows that the mass flow rate at the compressor inlet $\dot{m}_{in,suc} = -\dot{m}_{gsk} + \dot{m}_{in,i}$. The heat transfer rate $\dot{Q}_{amb,suc}$ is evaluated by assuming that $h_{in,i} = h_{in,suc}$.

The energy balance in the discharge chamber is represented as follows:

$$\dot{Q}_{amb,dis} = \dot{m}_{out,i}\, h_{out,i} - \dot{m}_{fo}\, h_{fo} - \dot{m}_{out,dis}\, h_{out,dis}. \quad \text{Eq. (8)}$$

where $\dot{m}_{out,i}$ and $h_{out,i}$ are evaluated with the CC model and $\dot{m}_{fo}$ is obtained from the relationship developed for the restrictor channels model. The term $\dot{Q}_{amb,dis}$ is determined to satisfy $h_{fo} = h_{out,dis}$.It should be noted that since the suction and discharge systems are considered to be adiabatic, $\dot{Q}_{amb,suc}$ can be regarded as the energy loss, or inefficiency, brought about by the leakage of gas that reach the suction system, whereas $\dot{Q}_{amb,dis}$ represents the energy loss due to the amount of gas fed into the piston-cylinder clearance from the discharge system through the restrictor channels. Replacing the definitions of isentropic power, $\dot{W}_s = \dot{m}\left(h_{out,dis} - h_{in,suc}\right)$, and isentropic efficiency, $\eta_s = \dot{W}_s/\dot{W}$, in Eq. (6) gives:

$$\frac{1}{\eta_s} - 1 = \frac{\dot{Q}_{amb,gap}}{\dot{W}_s} + \frac{\dot{Q}_{amb,suc}}{\dot{W}_s} + \frac{\dot{Q}_{amb,dis}}{\dot{W}_s} \quad \text{Eq. (9)}$$

Defining the parameter εs_k to represent the increase in power input, i.e., isentropic inefficiency, due to the specific effect k ($\varepsilon s_k = \dot{Q}_k/\dot{W}_s$):

$$\varepsilon s = \varepsilon s_{amb,gap} + \varepsilon s_{amb,suc} + \varepsilon s_{amb,dis} \quad \text{Eq. (10)}$$

Therefore, the total isentropic inefficiency, εs, is associated with the heat rejection rates in the piston-cylinder clearance ($\varepsilon s_{amb,gap}$), suction chamber ($\varepsilon s_{amb,suc}$) and discharge chamber ($\varepsilon s_{amb,dis}$). By combining Eqs. (9) and (10), one obtains $\eta_s = 1/(1 + \varepsilon s)$.

4. RESULTS

All simulations carried out in the present study considered the evaporating pressure of 114.8 kPa. Considering R134a as the refrigerant fluid, the evaporating temperature is 249.85 K. Moreover, based on experimental data, the temperature of the gas at the compressor inlet was prescribed as 305.15 K and the temperatures of the piston and cylinder walls were set at 328.15 K. A preliminary study was performed to verify the time and space discretization errors of the PCC model, following the Richardson extrapolation method (Cadafalch et al., 2002). The PCC model was then validated through comparisons with data from the literature (Suefuji et al., 1992) for different values of clearance and pressure ratio, with a mean difference of 14% being observed.

4.1. Baseline Operating Conditions

Firstly, results were obtained under the baseline operating conditions defined by the following parameters: Π = 8.97; p_{cond} = 1030.3 kPa; T_{cond} = 313.65K; δ = 5μm; f = 120Hz; and L_{amp}/L_{cyl} = 0.215. Data presented in Table 2 indicate a reduction of 54.0% in the mass flow rate due to the dead volume brought about by the small amplitude of L_{amp}/L_{cyl} for the baseline operating conditions. The volumetric inefficiency resulting from the flow in the piston-cylinder clearance (εv) is only 0.79%, mostly attributed to the inefficiencies $\varepsilon v_{gtp,suc}$ and $\varepsilon v_{gtp,exp}$ associated with leakage through the top gap ($\dot{m}_{gtp}$) during the expansion and suction processes. The results for the compressor power, isentropic efficiency and inefficiencies are reported in Table 3. The total inefficiency, εs,

increased the power consumption ($\dot{W}_{ind} + \dot{W}_f$) by 1.41% with reference to the isentropic power $\dot{W}_s$. Only 0.21% of this value is due to the piston friction power $\dot{W}_f$, also referred to as mechanical loss. On the other hand, the compression efficiency, η_c, undergoes a more significant change, greater than 1%.

Table 3 also shows that the main factor responsible for the increase in the energy consumption is the viscous dissipation in the piston-cylinder clearance ($\varepsilon s_{amb,gap}$). The results for the viscous dissipation rate (Φ) predicted by the PCC model during the compression cycle showed the peak for Φ occurs close to the TDC. At this position the pressure is highest and hence the same occurs with the velocity magnitudes and gradients in the piston-cylinder clearance. The mean value for Φ calculated over the cycle is 0.69 W, which corresponds to 75% of the energy that enters the gap (= 0.92W) during the compression cycle. Fig. 4 presents the corresponding velocity field in the midplane of the piston-cylinder clearance for different instants of time. The oscillatory behavior of the flow is evident, with the highest velocity magnitudes occurring in the piston top gap close to the TDC, when the pressure inside the compression chamber reaches its highest value. These high levels of velocity increase the viscous dissipation in the piston-cylinder clearance.

Table 2: Mass flow rates and different sources of volumetric inefficiency.

Parameter	Value	Parameter	Value	Parameter	Value
$\dot{m}_{th}$ [kg/s]	2.20E-03	εv_{idc} [-]	53.96%	$\varepsilon v_{gtp,exp}$ [-]	0.39%
$\dot{m}$ [kg/s]	9.96E-04	εv_{gsk} [-]	0.21%	εv_{sh} [-]	0.01%
η_v [-]	45.25%	$\varepsilon v_{gtp,suc}$ [-]	0.18%	εv [-]	0.79%

Table 3: Power input and different sources of isentropic inefficiency.

Parameter	Value	Parameter	Value	Parameter	Value
$\dot{W}_s$ [W]	60.65	η_c [-]	98.81%	$\varepsilon s_{amb,gap}$ [-]	1.15%
$\dot{W}_{ind}$ [W]	61.37	η_{mec} [-]	99.79%	εs [-]	1.41%
$\dot{W}_f$ [W]	0.13	$\varepsilon s_{amb,suc}$ [-]	0.14%	Φ [W]	0.69
η_s [-]	98.61%	$\varepsilon s_{amb,dis}$ [-]	0.12%		

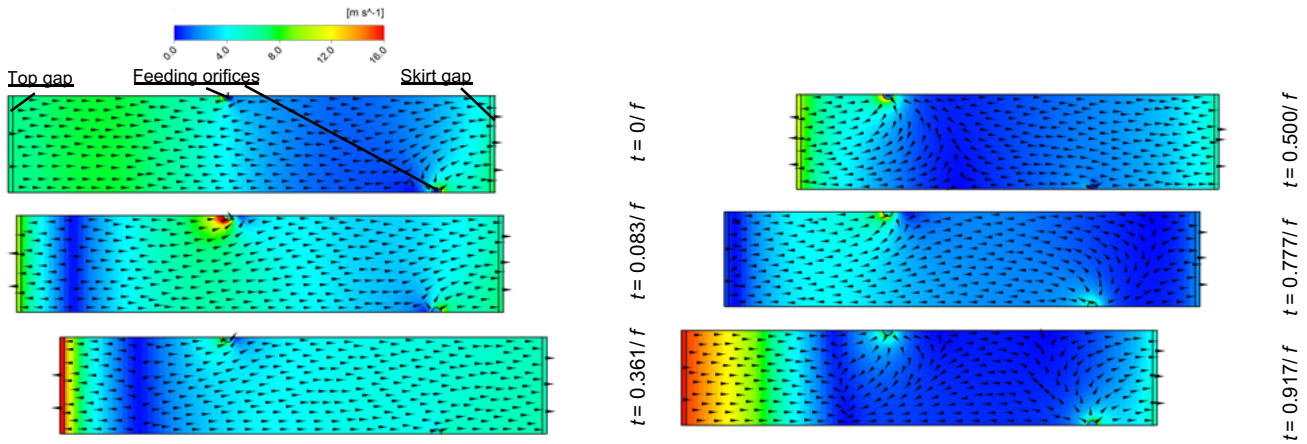

Figure 4: Velocity field in the piston-cylinder clearance.

4.2. Parametric Analysis

The compressor performance and thermodynamic inefficiencies were analyzed by varying four parameters: operating frequency (f), amplitude of oscillation (L_{amp}), pressure ratio (Π) and piston-cylinder radial clearance (δ). Each of these parameters was varied individually, while for the others the values adopted for the baseline operating conditions were maintained. The compressor efficiency was found to be mainly affected by the clearance and pressure ratio. Due to space restriction, we report only the results for the piston-cylinder radial clearance (δ), which was evaluated for six values: δ = 2.5, 3.0, 4.0, 5.0, 7.5 and 10.0 μm.

According to Table 4, the volumetric efficiency undergoes a reduction of 2.5% ($\eta_v - \eta_{v,idc}$) and the compression and isentropic efficiencies decrease by more than 4% when the clearance is varied from 2.5 μm to 10.0 μm. Fig. 5(a) shows that all volumetric inefficiencies increase with the piston-cylinder clearance. In particular, the increase in the leakage through the skirt gap (εv_{gsk}) is a direct result of the greater leakage at the top gap ($\varepsilon v_{gtp,exp}$ and $\varepsilon v_{gtp,suc}$), since the mass flow rate through the feeding orifices does not vary with δ.

The results in Fig. 5(b) indicate that the effect of the viscous dissipation inside the piston-cylinder clearance, $\varepsilon s_{amb,gap}$, is the most significant isentropic inefficiency. The leakage through the skirt gap is considerably increased with the clearance and therefore the same occurs with the heat rejection rate in the suction environment ($\dot{Q}_{amb,suc}$) and the inefficiency $\varepsilon s_{amb,suc}$. We found that, of the parameters considered in this analysis, the radial clearance has the greatest effect on the volumetric and isentropic inefficiencies. Small clearances are associated with greater frictional power, $\dot{W}_f$, due to the resistive viscous force on the piston wall. However, the effect of greater leakage as the radial clearance δ is increased results in a negative trade-off and the compressor efficiency is decreased.

Table 4: Numerical results as a function of radial clearance.

δ [μm]	2.5	3.0	4.0	5.0	7.5	10.0
$\dot{m}$ [kg/s]	1.01E-03	1.01E-03	1.00E-03	9.96E-04	9.80E-04	9.54E-04
$\dot{W}_{ind}$ [W]	61.84	61.76	61.63	61.50	61.36	61.20
$\dot{W}_f$ [W]	0.21	0.18	0.15	0.13	0.11	0.11
η_v [-]	45.73%	45.64%	45.45%	45.25%	44.47%	43.28%
$\eta_{v,idc}$ [-]	46.04%	46.04%	46.04%	46.04%	46.04%	46.04%
η_s [-]	99.13%	99.07%	98.87%	98.61%	97.19%	94.91%
η_c [-]	99.47%	99.36%	99.11%	98.81%	97.37%	95.08%

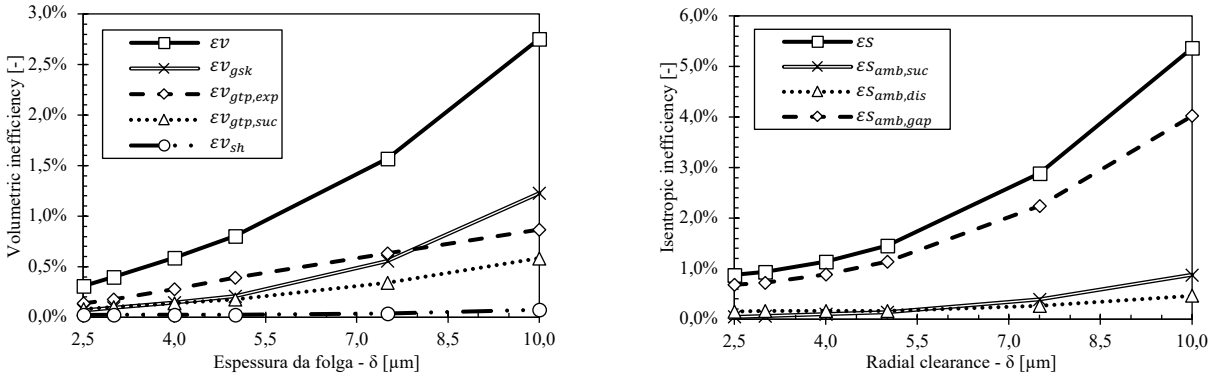

(a) (b)

Figure 5: (a) Volumetric and (b) isentropic inefficiencies as a function of radial clearance.

5. CONCLUSION

A convenient method was adopted to identify different sources of the thermodynamic inefficiency in the piston-cylinder clearance of an oil-free linear compressor. The leakage that occurs from the top gap to the compression chamber during the expansion and suction processes was found to significantly reduce the amount of mass of refrigerant that can enter the compression chamber through the suction valve. The mechanical energy dissipated by viscous friction in the clearance is the most influential source of isentropic inefficiency, whereas the viscous friction force on the piston has a negligible effect. The compressor efficiency was found to be mainly affected by the clearance and pressure ratio. A reduction of 2.5% in the volumetric efficiency and 4.2% in the isentropic efficiency, for instance, were predicted when the clearance was varied from 2.5 μm to 10.0 μm.

ACKNOWLEDGEMENTS

The present study was developed as part of a technical-scientific cooperation program between the Federal University of Santa Catarina and Nidec-GA (Embraco). Financial support was provided by the National Institutes of Science and Technology (INCT) Program (CNPq Grant No. 443696/2014-4; FAPESC Grant No. 2018TR1576). Additional funding from EMBRAPII Unit POLO/UFSC and CAPES is duly acknowledged.

NOMENCLATURE

D_{cap}	restrictor channel diameter (m)	Es	isentropic inefficiency (-)
D_{pist}	piston diameter (m)	η_c	overall efficiency (-)
F	operating frequency (s^{-1})	η_{ele}	electrical efficiency (-)
h	specific enthalpy ($J \times kg^{-1}$)	η_{mec}	mechanical efficiency (-)
L_{amp}	piston oscillation amplitude (m)	η_s	isentropic efficiency (-)
L_{cap}	length of the restrictor channel (m)	η_v	volumetric efficiency (-)
L_{cfo}	length of the feeding hole (m)	$\eta_{v,idc}$	theoretical volumetric efficiency (-)
L_{cyl}	cylinder length (m)	ρ	density ($kg \times m^{-3}$)
L_{instop}	distance from datum to valve plate (m)		**Subscripts**
L_{pist}	piston length (m)	*amb*	chamber
$\dot{m}$	mass flow rate ($kg \times s^{-1}$)	*cyl*	cylinder
p	pressure (Pa)	*dis*	discharge
$\dot{Q}$	heat transfer rate (W)	*exp*	expansion
T	temperature (K)	*fo*	feeding orifice
T_{cond}	condensing temperature (K)	*gap*	piston cylinder clearance
T_{evap}	evaporating temperature (K)	*gsk*	piston skirt
T_{suc}	suction line temperature (K)	*gtp*	piston top
v	specific volume ($m^3 \times kg^{-1}$)	*i*	compression chamber
$\forall$	volume (m^3)	*in*	entering the control volume
$\dot{W}$	compressor power consumption (W)	*ini*	initial
$\dot{W}_f$	piston friction power consumption (W)	*manc*	aerostatic bearing
$\dot{W}_{ind}$	indicated power (W)	*out*	exiting the control volume
$\dot{W}_s$	isentropic power (W)	*pist*	piston
	Greek letters	*sh*	superheating
δ	piston-cylinder clearance (m)	*suc*	suction
εv	volumetric inefficiency (-)	*suc*	suction

REFERENCES

Bradshaw, C.R., Groll, E.A., Garimella, S.V., 2011. A comprehensive model of miniature-scale linear compressor for electronics cooling. Int. J. Refrigeration 34, 63–73.

Braga, V.M., Deschamps, C.J., 2017. Numerical analysis of gas leakage in the piston-cylinder clearance of reciprocating compressors considering compressibility effects. IOP Conf. Ser.: Mater. Sci. Eng. 232, 012006.

Cadafalch, J., Pérez-Segarra, C. D., Cònsul, R., Oliva, A., 2002. Verification of finite volume computations on steady-state fluid flow and heat transfer. J. Fluids Eng. 124, n. 1, 11-21.

Hülse, E.R., Prata, A.T., 2016. Numerical Modeling of Capillary Compensated Aerostatic Bearing Applied to Linear Reciprocating Compressor. Proc. Int. Compressor Engng. Conf. at Purdue.

Jomde, A., Anderson, A., Bhojwani, V., Kedia, S., Jangale, N., Kolas, K., Khedar, P., 2018. Modeling and measurement of a moving coil oil-free linear compressor performance for refrigeration application using R134a. Int. J. Refrigeration 88, 182-194.

Pérez-Segarra, C. D., Rigola, J., Sòria, M., Oliva, A., 2005. Detailed thermodynamic characterization of hermetic reciprocating compressors. Int. J. Refrigeration 28, 579-593.

Suefuji K., Shiibayashi M., Tojo K., 1992. Performance analysis of hermetic scroll compressor. Proc. Int. Compressor Engng. Conf. at Purdue.